ELECTRONIC SUPPLEMENTARY INFORMATION

Targeting of DNA molecules, BSA/*c*-Met tyrosine kinase receptor and anti-proliferative activity of bis(terpyridine)copper(II) complexes

Dharmasivam Mahendiran[a], Raju Senthil Kumar[b], Vijayan Viswanathan[c], Devadasan Velmurugan[c] and Aziz Kalilur Rahiman[*a]

[a]*Post-Graduate and Research Department of Chemistry, The New College (Autonomous), Chennai 600 014, India.*

[b]*Department of Pharmaceutical Chemistry, Swami Vivekanandha College of Pharmacy, Elayampalayam, Tiruchengodu 637 205, India.*

[c]*CAS in Crystallography and Biophysics, University of Madras, Guindy Campus, Chennai 600 025, India.*

Section 1

Chemical potential (μ) = $-\chi$ = $\frac{E_{LUMO} + E_{HOMO}}{2}$

Chemical hardness (η) = $\frac{E_{LUMO} - E_{HOMO}}{2}$

Electrophilicity (ω) = $\frac{\mu^2}{2\eta}$

The nuclear independent chemical shift (NICS)[1] values were calculated using the gauge-including atomic orbitals (GIAO) method at the B3LYP level of theory using Gaussian-03 software.

1. Z. Chen, C.S. Wannere, C. Corminboeuf, R. Puchta, and P.R. Schleyer, *Chem. Rev.,* 2005, **105,** 3842−3888.

Table S1 Selected bond lengths (Å) and bond angles (º) for complex **2**·CH_3OH·$(H_2O)_6$

Bond length (Å)	
N(1)–Cu	2.235(7)
N(2)–Cu	1.975(7)
N(3)–Cu	2.212(8)
N(4)–Cu	2.110(7)
N(5)–Cu	1.954(7)
N(6)–Cu	2.127(8)
Bond angle (°)	
C(5)–N(1)–Cu	113.6(5)
C(1)–N(1)–Cu	128.2(7)
C(6)–N(2)–Cu	122.0(6)
C(10)–N(2)–Cu	120.2(6)
C(11)–N(3)–Cu	112.7(6)
C(15)–N(3)–Cu	127.6(8)
C(23)–N(4)–Cu	126.4(7)
C(27)–N(4)–Cu	114.1(5)
C(28)–N(5)–Cu	119.8(5)
C(32)–N(5)–Cu	119.6(6)
C(33)–N(6)-Cu	114.0(6)
C(37)–N(6)–Cu	127.1(7)
N(5)–Cu–N(2)	178.6(3)
N(5)–Cu–N(4)	78.3(3)
N(2)–Cu–N(4)	100.7(3)
N(5)–Cu–N(6)	77.7(3)
N(2)–Cu–N(6)	103.4(3)
N(4)–Cu–N(6)	155.9(3)
N(5)–Cu–N(3)	101.8(3)
N(2)–Cu–N(3)	77.2(3)

Table S2 Hydrogen bonding parameters for complex **2**·CH_3OH·$(H_2O)_6$ [Å and °]

D-H···A	d(D-H) Å	d(H···A) Å	d(D···A) Å	(D-H···A)°
C(4)-H(4)···Cl(1)	0.93	2.69	3.620(12)	174
C(17)-H(17)···Cl(1)	0.93	2.74	3.620(17)	157
C(22)-H(22A)···Cl(2)#1	0.96	2.81	3.743(19)	166
C(23)-H(23)···O(2)#1	0.93	2.52	3.200(15)	130
C(34)-H(34)···Cl(2)	0.93	2.82	3.728(16)	167
C(43)-H(43)···Cl(2)	0.93	2.75	3.651(18)	165

Symmetry transformations used to generate equivalent atoms:

#1: 1–y, x–y, –1/3+z

Table S3 The optimized geometrical parameters of bis(terpyridine)copper(II) complexes (**1**−**5**) in the ground state at the B3LYP/LANL2DZ level, together with the crystal data of **2**

Bond length (Å)	Calculated					Experimental
Complexes	1	2	3	4	5	2
Cu–N1	2.243	2.243	2.127	2.100	2.182	2.235(7)
Cu–N2	1.912	1.984	1.932	1.983	1.980	1.975(7)
Cu–N3	2.118	2.218	2.121	1.983	2.212	2.212(8)
Cu–N4	2.136	2.121	2.113	2.102	2.047	2.110(7)
Cu–N5	2.180	2.139	2.120	1.893	1.900	1.954(7)
Cu–N6	2.276	2.238	2.289	2.021	2.012	2.127(8)
Bond angle (deg)						
C(5)−N(1)−Cu	113.1	113.7	112.8	113.9	112.9	113.6(5)
C(1)−N(1)−Cu	126.8	126.2	126.5	126.9	125.9	128.2(7)
C(6)−N(2)−Cu	120.8	120.1	120.3	120.9	120.0	122.0(6)
C(10)−N(2)−Cu	117.3	118.6	118.1	118.9	117.8	120.2(6)
C(11)−N(3)−Cu	109.4	112.7	110.2	107.6	107.1	112.7(6)
C(15)−N(3)−Cu	134.2	128.2	132.9	122.4	139.7	127.6(8)
C(27)−N(4)−Cu	121.1	114.0	109.2	111.0	126.4	114.1(5)
C(23)−N(4)−Cu	127.9	127.5	121.3	112.3	134.6	126.4(7)
C(28)−N(5)−Cu	124.8	123.1	118.2	121.3	121.9	119.8(5)
C(32)−N(5)−Cu	103.3	122.0	134.5	142.5	120.4	119.6(6)
C(37)−N(6)−Cu	132.2	129.2	127.4	127.9	128.6	127.1(7)
C(33)−N(6)−Cu	113.9	111.3	117.2	109.3	121.4	114.0(6)
N(5)–Cu–N(2)	163.8	179.2	186.3	192.4	181.3	178.6(3)
N(5)–Cu–N(4)	69.3	77.2	82.0	86.8	77.2	78.3(3)
N(2)–Cu–N(4)	89.2	101.3	92.1	90.2	99.9	100.7(3)
N(5)–Cu–N(6)	80.3	79.3	91.0	86.3	81.2	77.7(3)
N(2)–Cu–N(6)	104.4	102.6	108.3	107.2	96.4	103.4(3)
N(4)–Cu–N(6)	160.1	153.7	148.9	159.3	147.3	155.9(3)
N(5)–Cu–N(3)	98.5	102.9	101.2	108.3	106.2	101.8(3)

N(2)–Cu–N(3)	56.3	75.8	62.4	71.0	74.4	77.2(3)

Table S4 The energy of experimental absorption bands and the electronic transitions calculated with the TD-DFT method for complexes **1**−**3**

Complexes	E (eV)	(*f*)	Wavelength (λ), nm		Major contributions
			Calc.	Exp.	
1	1.39	0.0026	746.25	716	HOMO→LUMO+2 (34%) HOMO−2→LUMO+2 (2%)
	1.51	0.0039	556.64	526	HOMO−1→LUMO (14%), HOMO→LUMO+1 (36%) HOMO−LUMO (3%)
	1.75	0.0047	346.31	338	HOMO→LUMO (40%) HOMO−2→LUMO+2 (4%), HOMO−1→LUMO (2%), HOMO−1→LUMO+1 (7%), HOMO→LUMO+1 (3%)
	2.01	0.0002	297.63	−	HOMO−2→LUMO+2 (27%), HOMO−1→LUMO+2 (14%) HOMO−1→LUMO (2%)
	2.68	0.0008	271.33	286	HOMO−2→LUMO+2 (51%) HOMO−1→LUMO (2%), HOMO−1→LUMO+2 (8%)
	3.42	0.0002	227.42	−	HOMO−1→LUMO (60%), HOMO→LUMO+1 (31%) HOMO−1→LUMO+2 (5%)
2	1.64	0.0004	748.32	747	HOMO→LUMO (15%) HOMO−2→LUMO (9%)
	2.00	0.0001	558.01	516	HOMO−2→LUMO (72%) HOMO−2→LUMO+1 (3%)
	2.27	0.0005	348.04	337	HOMO−1→LUMO (24%) HOMO−1→LUMO+1 (6%)
	2.79	0.0054	293.27	−	HOMO−1→LUMO+2 (47%), HOMO→LUMO+1 (21%)
	3.26	0.005	272.23	285	HOMO−1→LUMO+1 (41%), HOMO→LUMO+2 (13%)
	5.80	0.0009	226.64	−	HOMO−1→LUMO+1(A) (27%), HOMO→LUMO+1 (14%), HOMO→LUMO+2 (51%), HOMO−1→LUMO+2 (6%)
3	1.62	0.0005	749.63	743	HOMO→LUMO (15%)
	1.88	0.0001	546.82	519	HOMO−2→LUMO (78%) HOMO−2→LUMO+1 (5%)
	2.21	0.0009	348.89	327	HOMO−1→LUMO (23%), HOMO−1→LUMO+1 (11%)
	2.73	0.005	289.04	286	HOMO−1→LUMO+2 (45%), HOMO→LUMO+1 (24%)
	3.57	0.0042	271.54	−	HOMO−1→LUMO+1 (28%), HOMO→LUMO+2 (21%)
	5.71	0.0005	221.54	−	HOMO−1→LUMO+1 (34%), HOMO→LUMO+1 (12%), HOMO→LUMO+2 (46%) HOMO−1→LUMO+2 (6%)

Table S5 Electrochemical parameters for bis(terpyridine)copper(II) complexes (**1–5**)

Complexes	i_{pc} (10^{-5} A)	E_{pc} (V)
1	3.30	–0.771
2	4.73	–0.766
3	3.84	–0.783
4	2.86	–0.738
5	3.21	–0.743

Table S6 Molecular docking parameters of the bis(terpyridine)copper(II) complexes (**1**−**5**) with DNA

Complexes	Final intermolecular energy (kcal mol $^{-1}$)		Total (1)	Final total internal energy (kcal mol^{-1}) (2)	Torsional free energy (kcal mol^{-1}) (3)	Unbound system's energy [= (2)] (kcal mol^{-1}) (4)	Estimated free energy of binding [(1) + (2) + (3) − (4)] (kcal mol^{-1})
	vdW + H bond + dissolving energy	Electrostatic energy					
1	−5.07	−0.32	−5.39	−0.51	+1.10	−0.43	−4.37
2	−5.16	−0.14	−5.31	−0.09	+0.55	−0.09	−4.76
3	−5.22	−0.12	−5.34	+0.00	+0.00	+0.00	−5.34
4	−4.89	−0.18	−5.07	−0.11	+0.98	−0.11	−4.09
5	−4.78	−0.12	−4.90	−0.08	+1.09	−0.08	−3.88

Table S7 Quenching constant (K_q), binding constant (K_{bin}), and number of binding sites (n) for the interactions of bis(terpyridine)copper(II) complexes **2** and **3** with BSA

Complexes	K_q (M^{-1})	K_{bin} (M^{-1})	'n' value
3	2.76×10^5	3.83×10^5	1.39

Table S8 Effect of bis(terpyridine)copper(II) complexes (**1**−**3**) on apoptosis of MCF−7 cells by Hoechst dye staining method

Complexes	Apoptosis (%)
Control	6.2 ± 0.87
1 (25 μM)	24.6 ± 1.67
1 (50 μM)	52.34 ± 2.53
2 (25 μM)	26.47 ± 2.13
2 (50 μM)	63.4 ± 5.8
3 (25 μM)	32.14 ± 1.41
3 (50 μM)	78.03 ± 2.31

Average of 3 determinations, 3 replicates

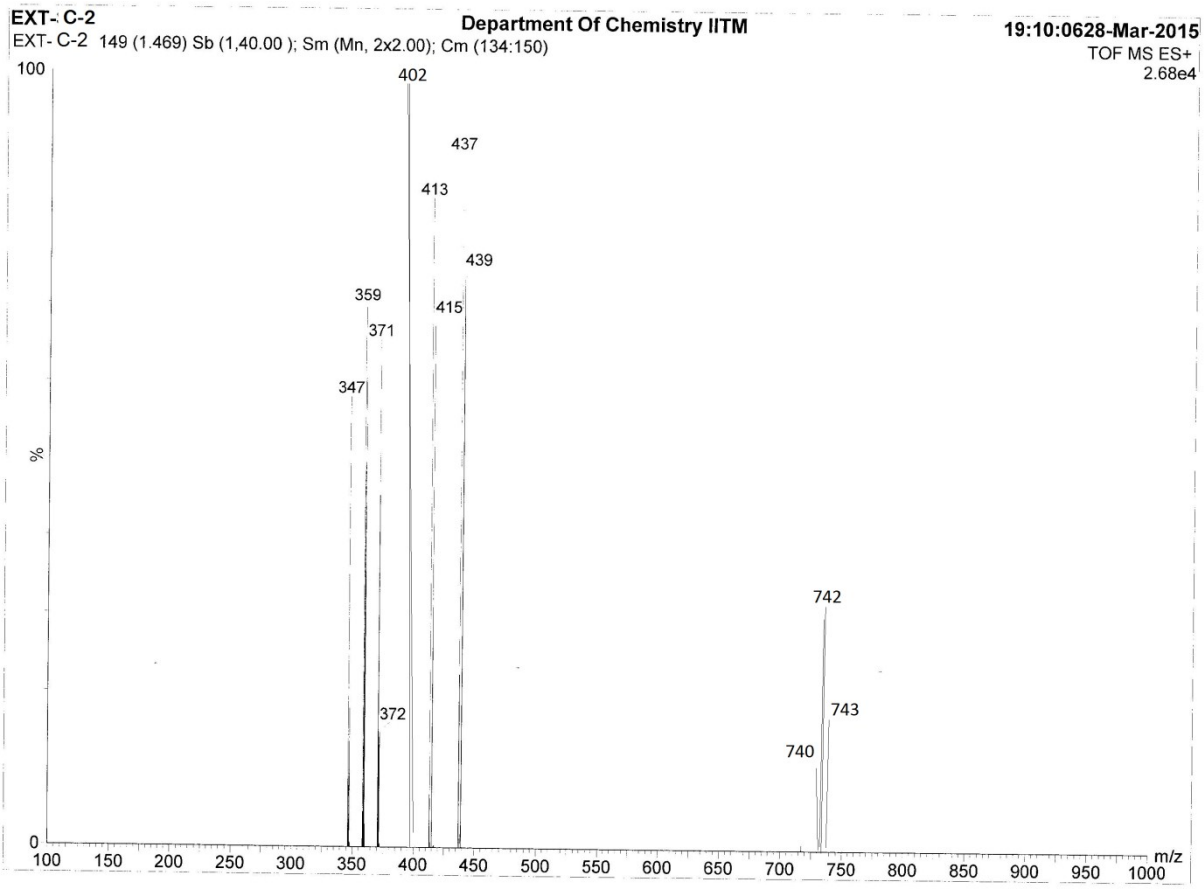

Fig. S1 ESI mass spectrum of bis(terpyridine)copper(II) complex **2**.

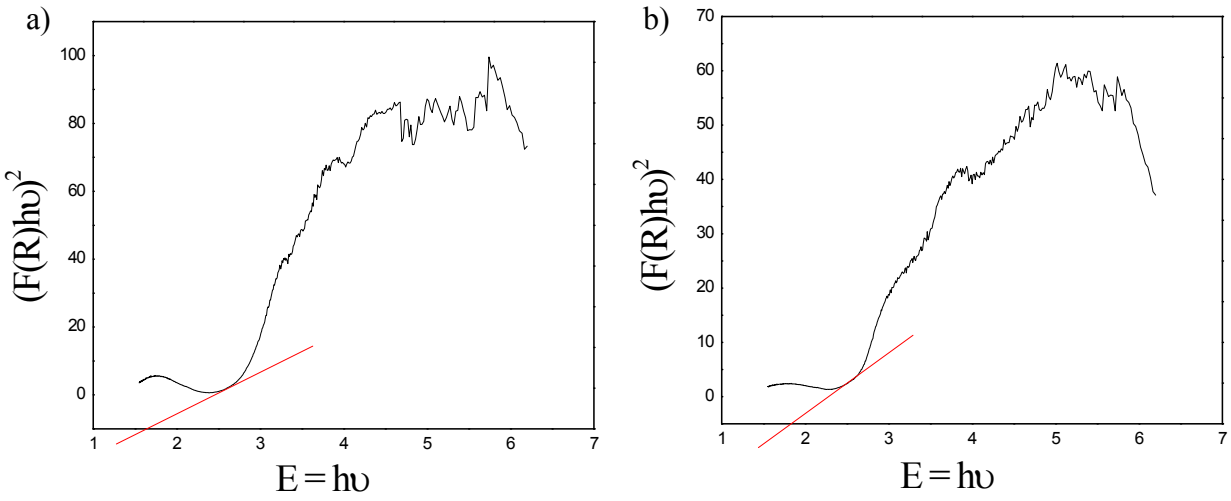

Fig. S2 Determination of the band-gap energy for bis(terpyridine)copper(II) complexes **1** (a) and **2** (b) from diffuse reflectance measurements.

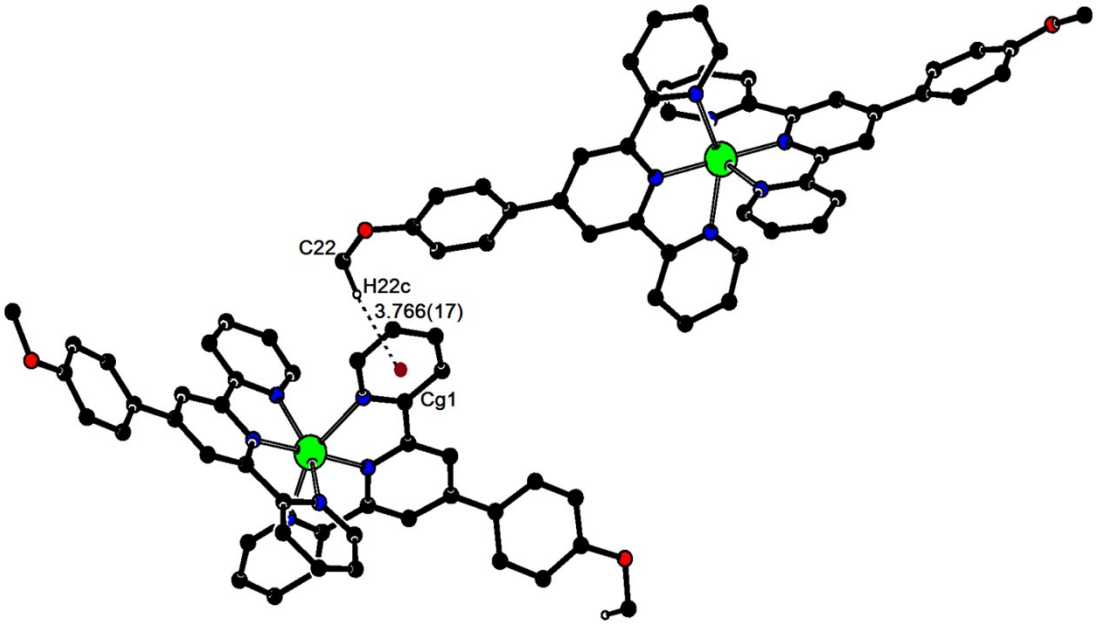

Fig. S3 C–H···π interaction of complex **2**·CH_3OH·$(H_2O)_6$.

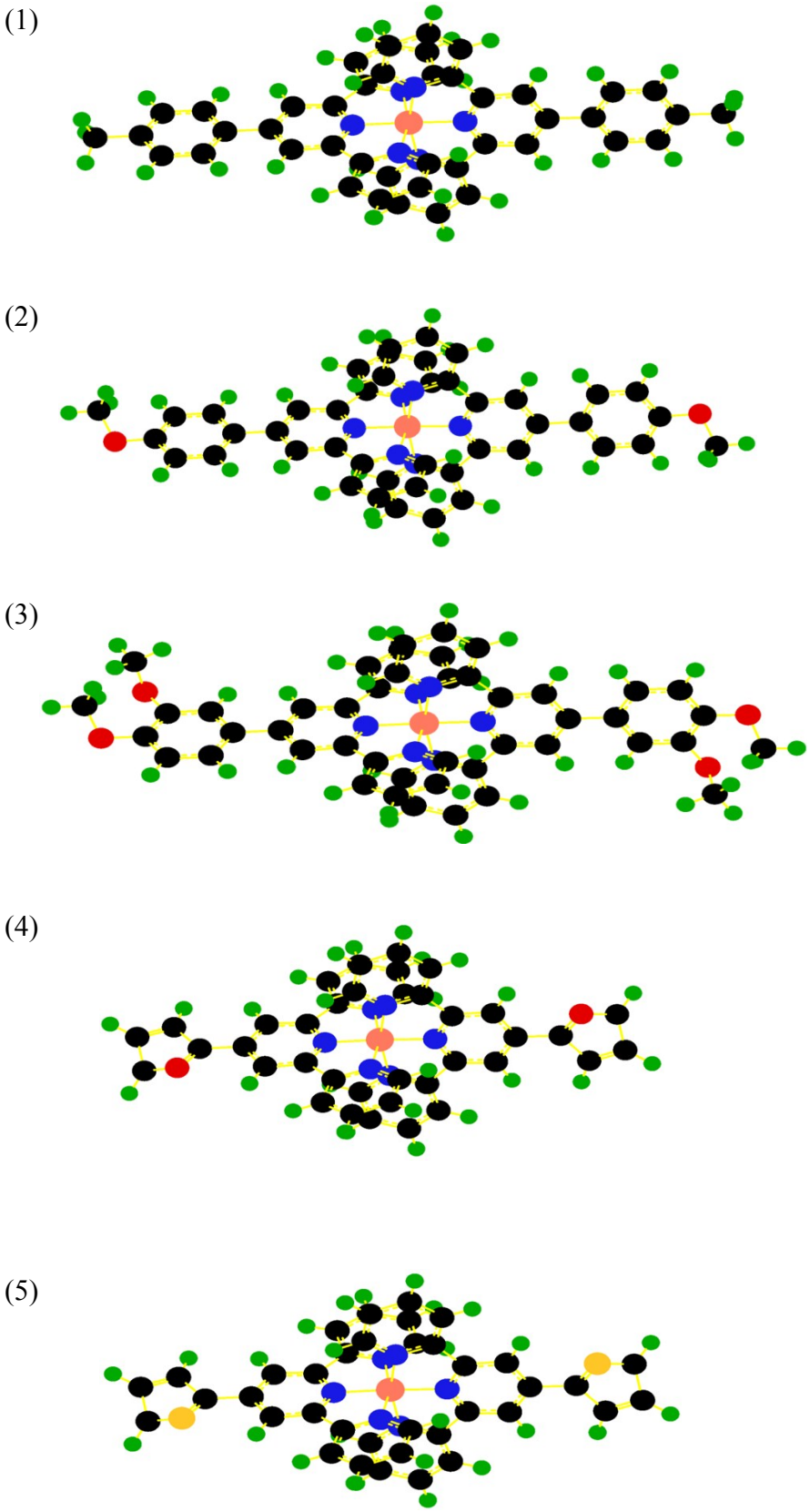

Fig. S4 Optimized geometries of the bis(terpyridine)copper(II) complexes **1**−**5**.

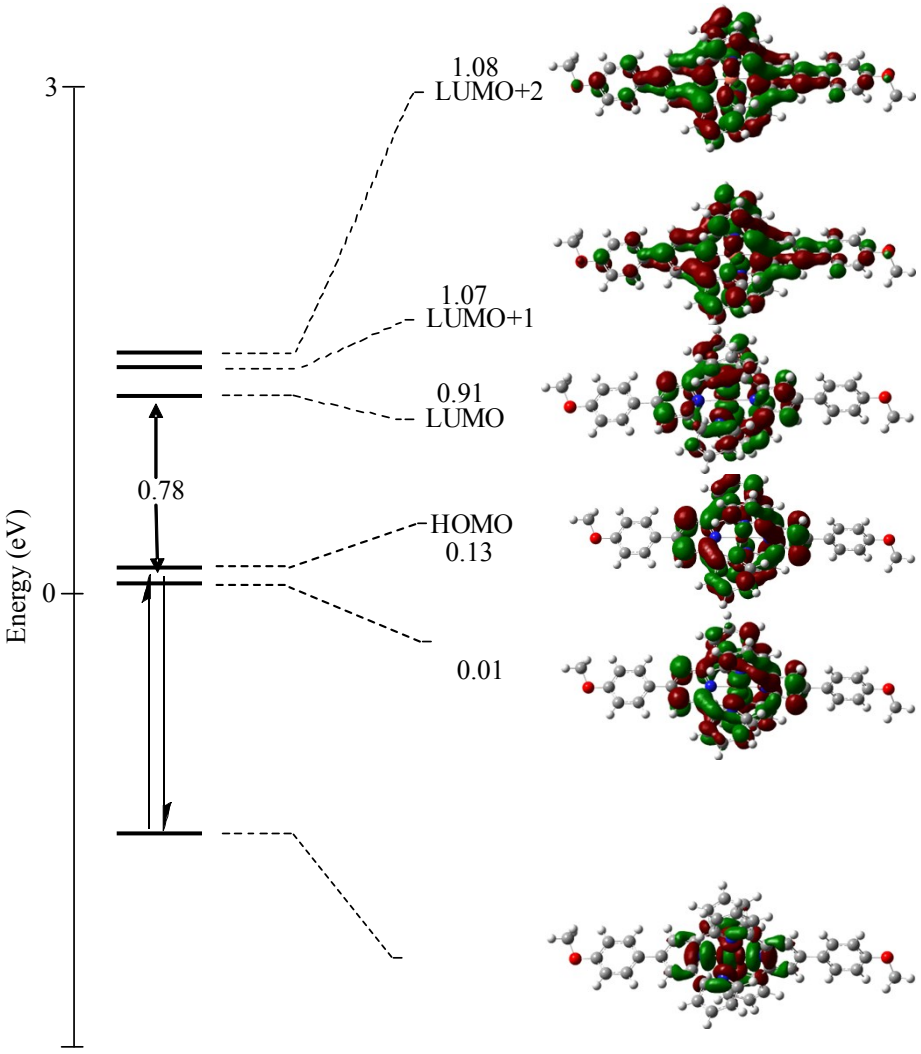

Fig. S5 Frontier MOs of bis(terpyridine)copper(II) complex **2**.

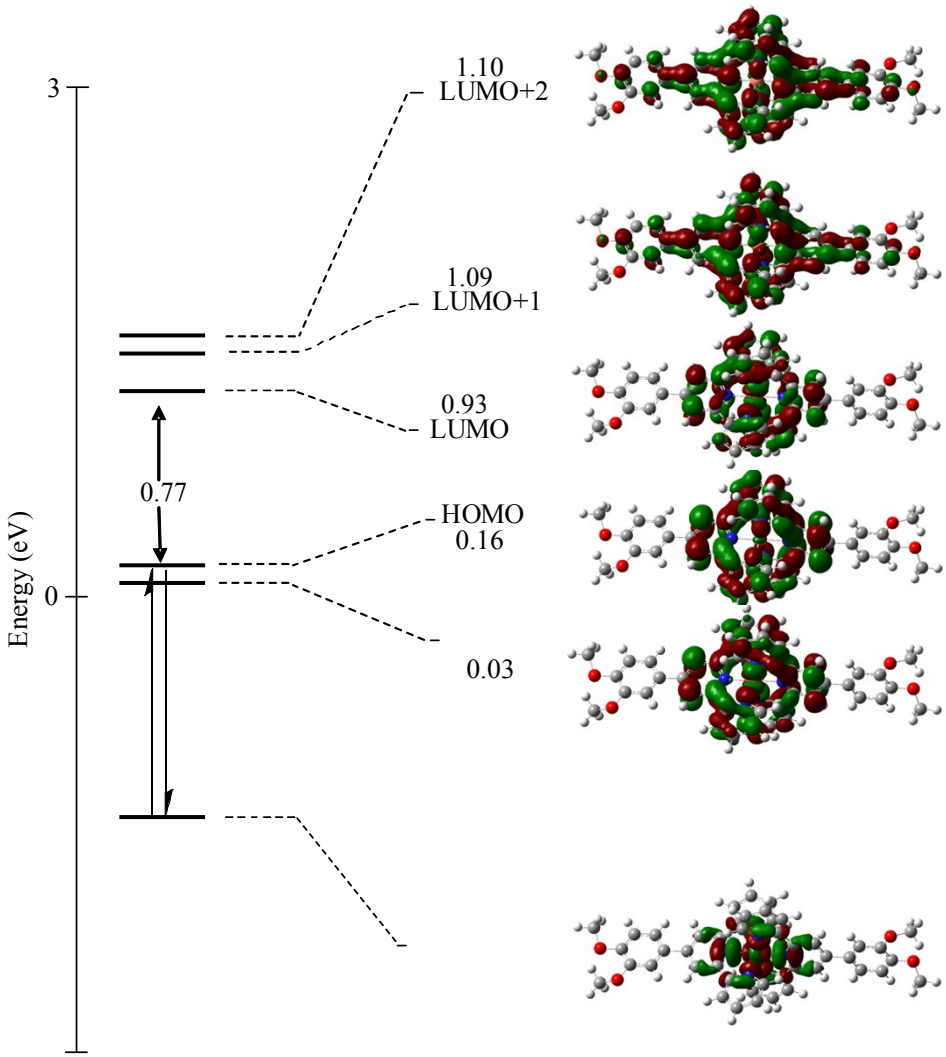

Fig. S6 Frontier MOs of bis(terpyridine)copper(II) complex **3**.

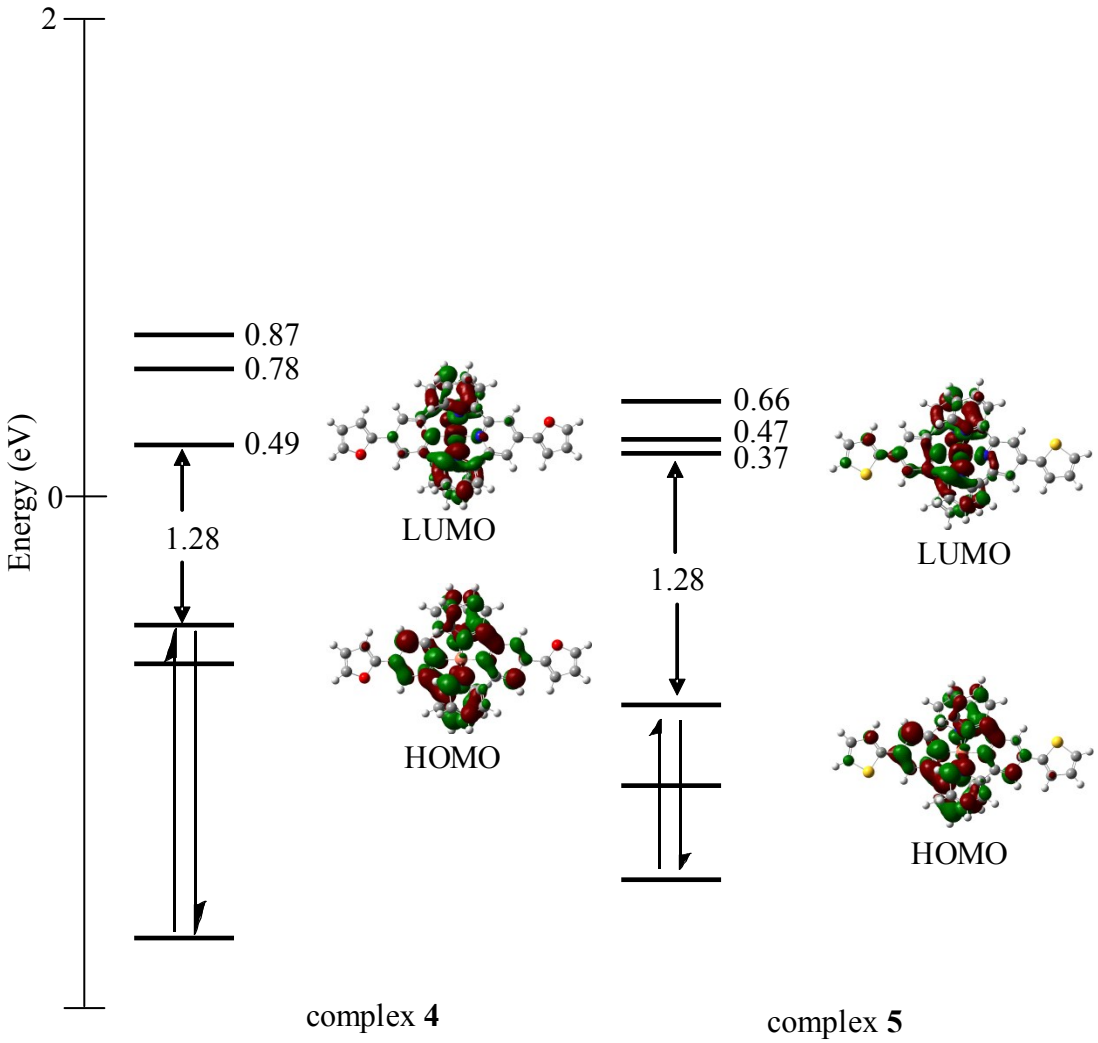

Fig. S7 Frontier MOs of bis(terpyridine)copper(II) complexes **4** and **5**.

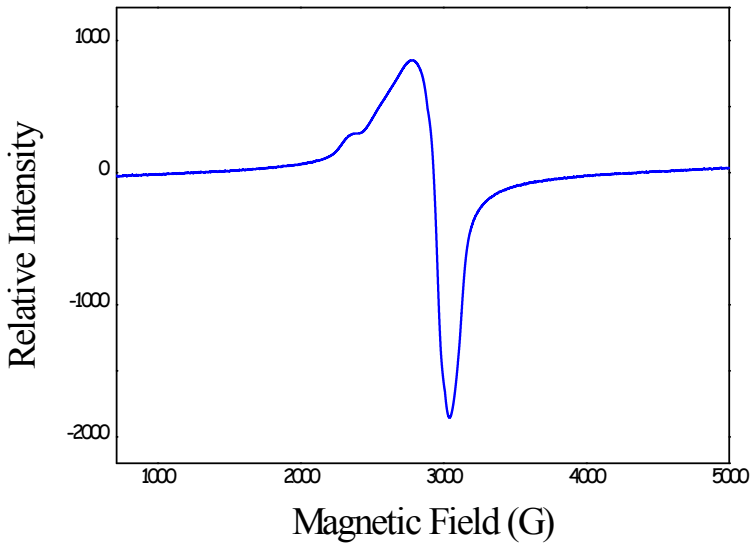

Fig. S8 Powder X-band EPR spectrum of bis(terpyridine)copper(II) complex **2**.

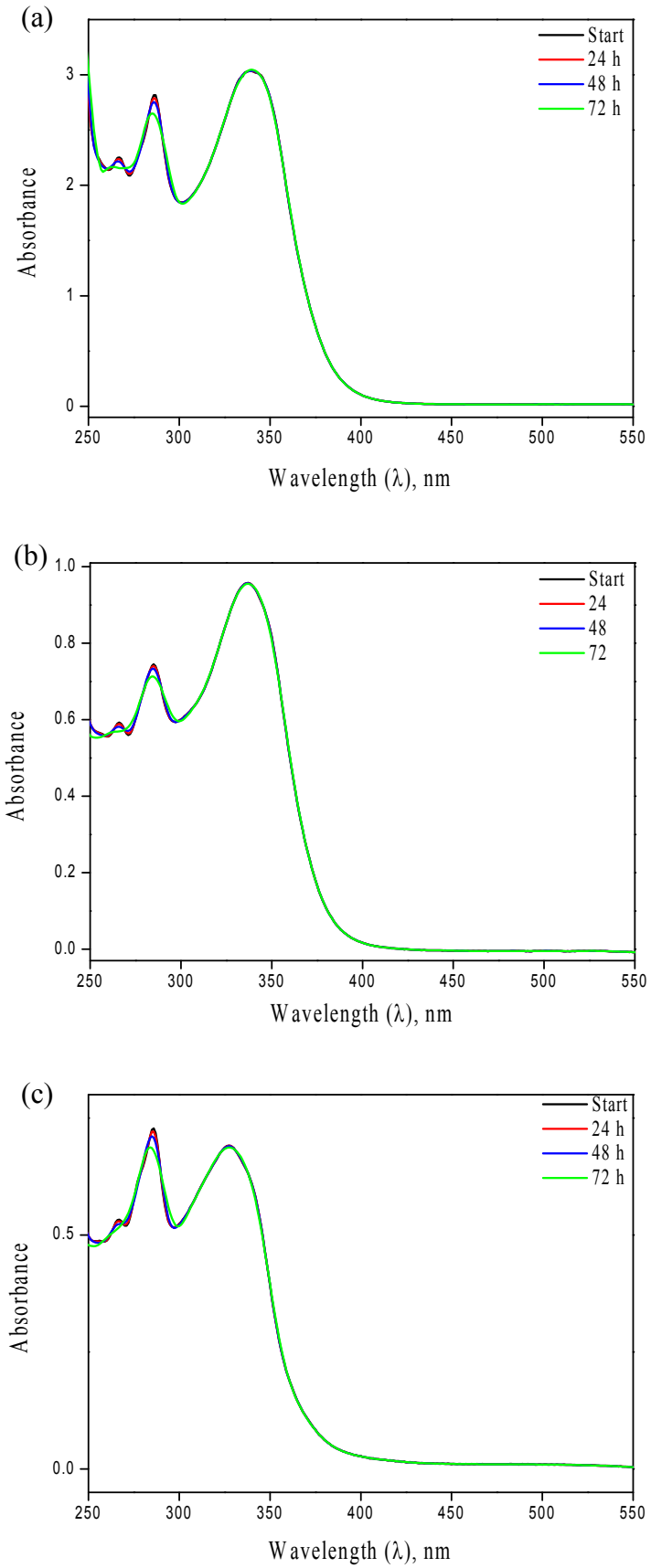

Fig. S9 Stability of bis(terpyridine)copper(II) complexes **1** (a), **2** (b) and **3** (c) measured by UV-Vis spectroscopy.

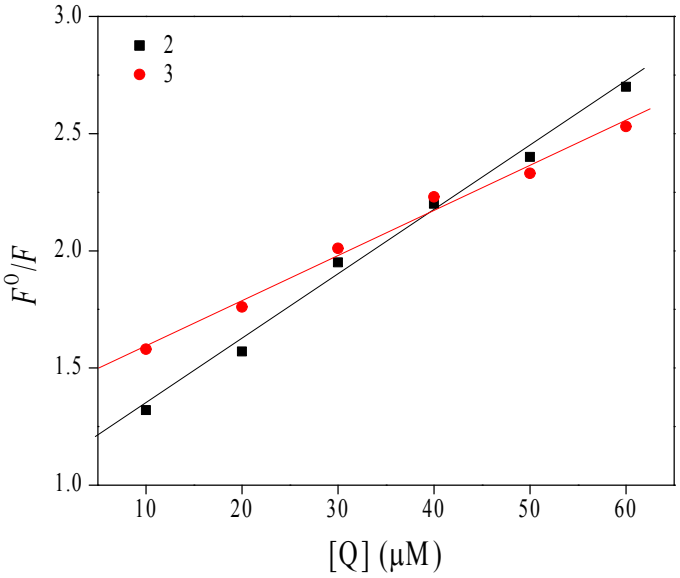

Fig. S10 Stern–Volmer plots of fluorescence titration of bis(terpyridine)copper(II) complexes **2** and **3** with CT–DNA.

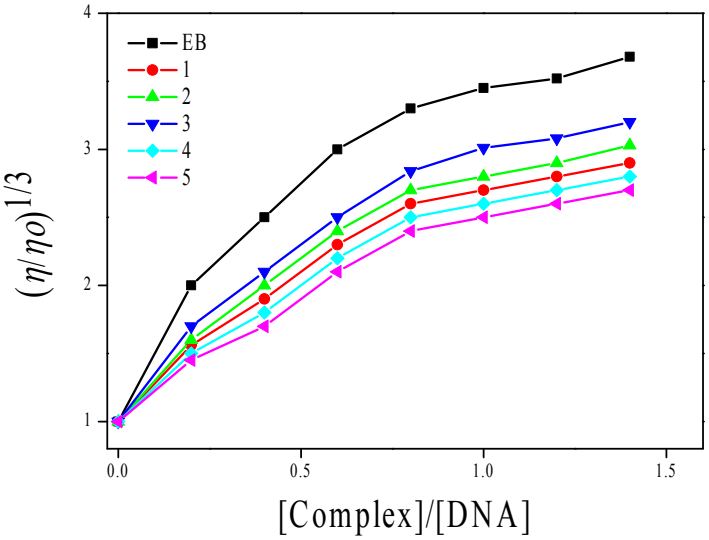

Fig. S11 Effect of bis(terpyridine)copper(II) complexes (**1–5**) on the viscosity of CT–DNA. Relative specific viscosity *versus* 1/*R* (*R* = [DNA]/[Complex], [DNA] = 200 μM, [Complex] = 10–100 μM).

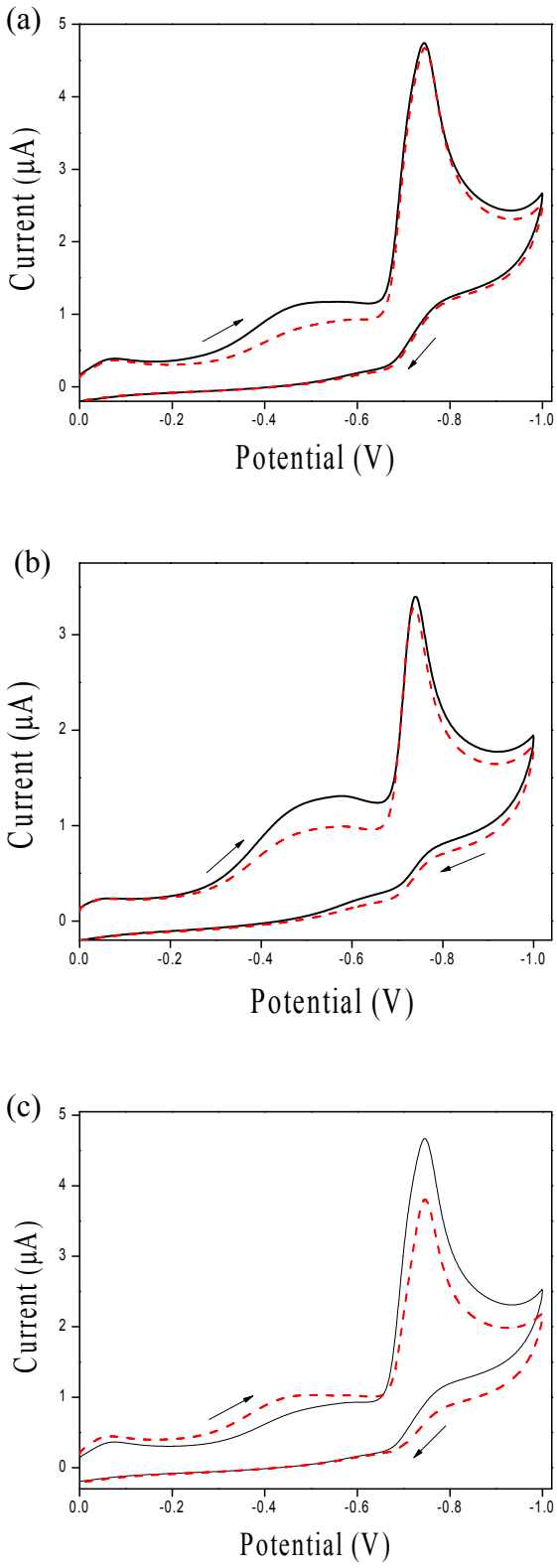

Fig. S12 Cyclic voltammograms of bis(terpyridine)copper(II) complexes **1** (a), **2** (b) and **3** (c) in DMF–Tris-HCl/NaCl buffer at pH 7.3 in the absence (solid line) and presence (dotted line) of CT–DNA and arrow indicates the current changes upon increasing DNA concentration.

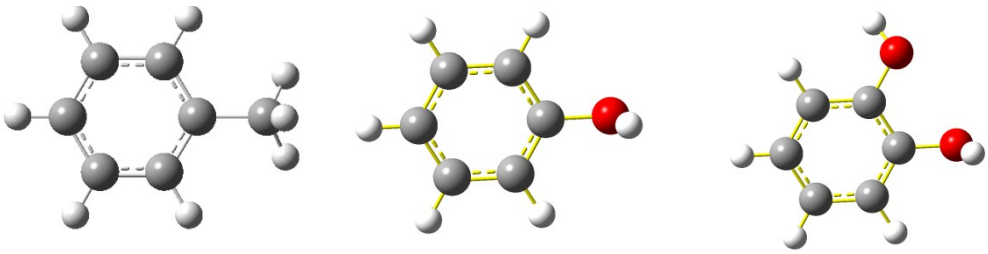

R1 R2 R3

Fig. S13 Optimized molecular structures of **R1** (toluene), **R2** (anisole) and **R3** (3,4-dimethoxybenzene) obtained from Gaussian 03W at the B3LYP/6-31G* level of calculation.

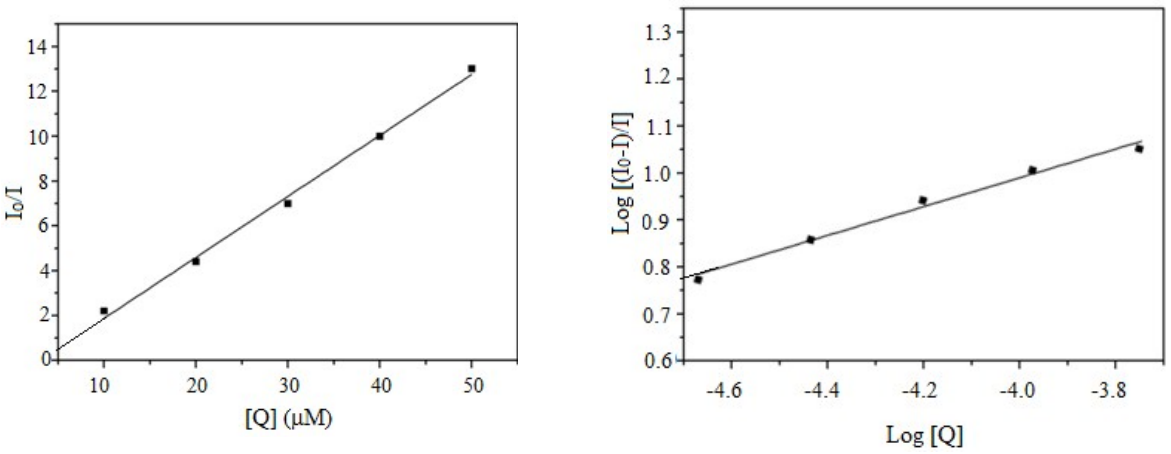

Fig. S14 Stern-Volmer plots and Scatchard plots of the fluorescence titration of the complex **3** with BSA.

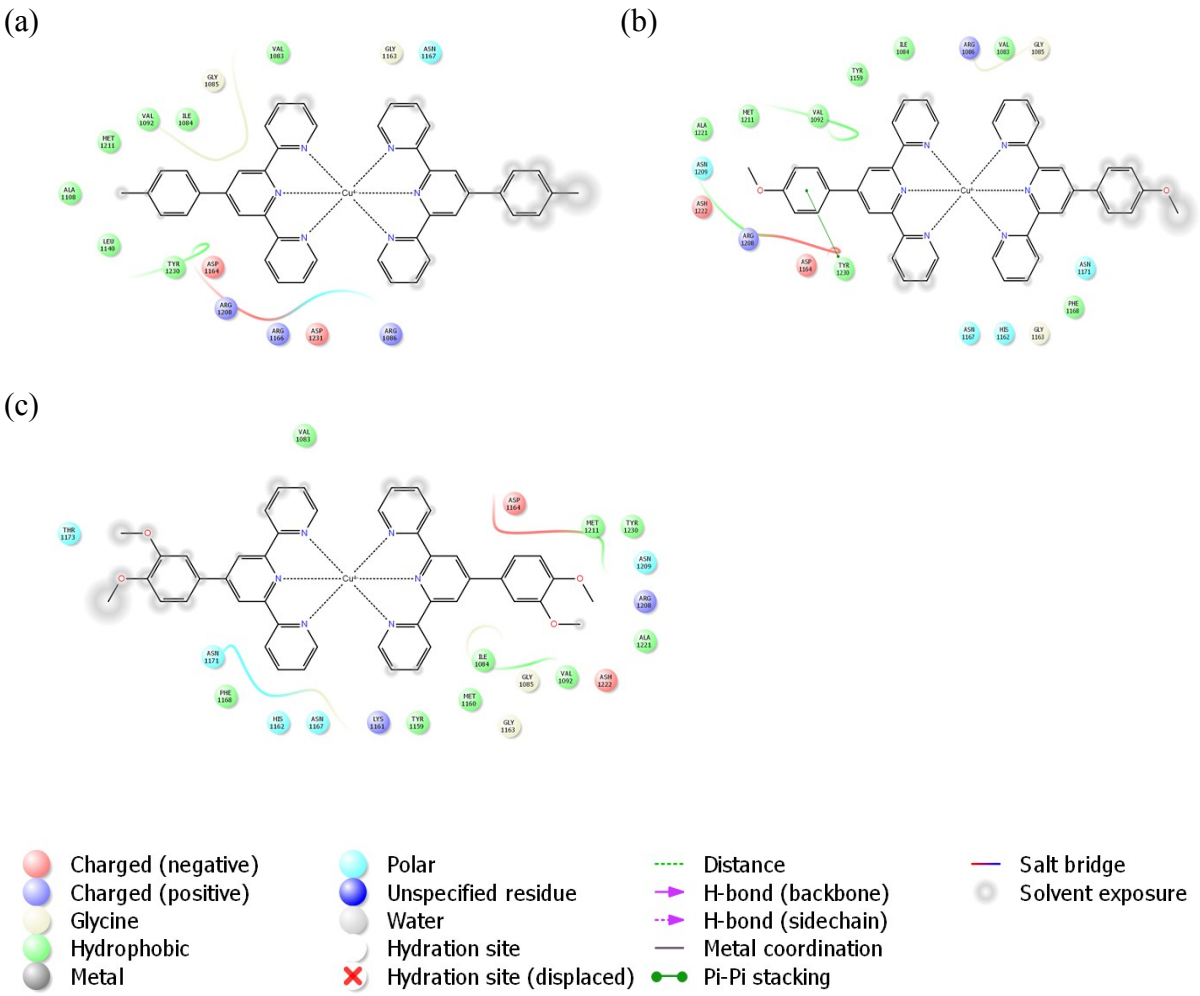

Fig. S15 Non-bonding interaction diagram of bis(terpyridine)copper(II) complexes **1** (a), **2 (b)** and **3** (c) docked with c-Met tyrosine kinase.

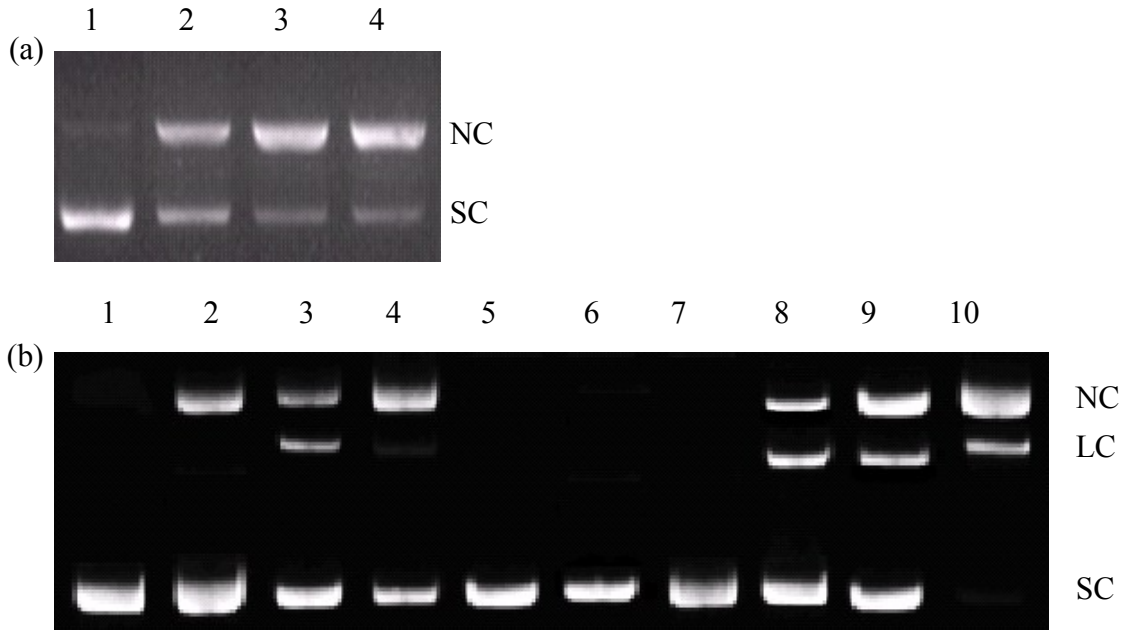

Fig. S16 (a) Gel electrophoresis diagram showing the cleavage of supercoiled pBR322 DNA (33.3 μM) by complexes **1–3** (10 μM) in the presence of H_2O_2 (40 μM): Lane 1: DNA control (33.3 μM); Lane 2–4: DNA + **1/2/3** + H_2O_2. (b) Analysis of the capacity of external additives in the presence of complexes **1–3**: Lane 1: DNA control, Lanes 2–4: DNA + **1**/**2/3** + NaN_3 (100 μM), Lanes 5-7: DNA + **1/2/3** + DMSO (4 μM), Lanes 8-10: DNA + **1/2/3** + SOD (1 U).